Metrol. Meas. Syst., Vol. 32 (2025) No. 4, pp. 1–16
DOI: 10.24425/mms.2025.155812

PAN POLSKA AKADEMIA NAUK

METROLOGY AND MEASUREMENT SYSTEMS

Index 330930, ISSN 0860-8229
www.metrology.wat.edu.pl

M&MS

FREQUENCY STABILITY OF SOFTWARE-DEFINED RADIOS – PART II. MODELING FOR SIMULATION STUDIES

Kacper Bednarz[1)], Jarosław Wojtuń[1)], Jan M. Kelner[1)], Cezary Ziółkowski[1)], Czesław Leśnik[2)]

1) Military University of Technology, Faculty of Electronics, Institute of Communications Systems, ul. gen. Sylwestra Kaliskiego 2, 00-908 Warsaw (✉ *jaroslaw.wojtun@wat.edu.pl*)
2) Military University of Technology, Faculty of Electronics, Institute of Radioelectronics, ul. gen. Sylwestra Kaliskiego 2, 00-908 Warsaw

Abstract

In the first part of this paper, we measured the frequency stability of widely available software-defined radio (SDR) platforms. The second part focuses on the problem of modeling the frequency instability of these devices, which is necessary in the process of designing new applications using simulation studies. This modeling is based on the measurement results obtained in the first part. For this purpose, the nature of changes in the instantaneous frequency of the received signal as a function of time is analysed, separating them into two parts, *i.e.*, a slow-changing trend and a fast-changing random component. A method of estimating the trend and fitting the normal distribution to fast frequency fluctuations is proposed to model the instantaneous frequency changes for several popular SDRs (including ADALM-PLUTO, B200mini, bladeRF, and USRP). The assumption about normal distribution for fast fluctuations is verified using the chi-square test. The models obtained enable the generation of signals in simulation studies that realistically represent the frequency variability observed in the measurements. The proposed approach enables simulation tests on SDR-based solutions, considering the impact of frequency instability without conducting long-standing or complex laboratory experiments.

Keywords: software-defined radio (SDR), frequency stability, measurement, modeling.

1. Introduction

In recent years, *software-defined radio* (SDR) has become one of the most important technologies in modern wireless communications. Its ability to implement most radio functions in software provides exceptional flexibility and adaptability compared to traditional hardware-based architectures [1, 2]. Continuous progress in *digital signal processing* (DSP) and computing power has allowed SDRs to play a crucial role in various domains, including consumer electronics, commercial telecommunications, defense, and scientific research [3, 4].

Article history: received April 24, 2025; revised July 13, 2025; accepted October 2, 2025; available online November 27, 2025.

Thanks to reconfigurability, compact size, and low power consumption, SDR platforms are now widely used in battery-powered systems, sensor networks, and mobile devices [5]. Moreover, SDRs allow for the implementation of advanced signal processing algorithms, directly improving the quality and reliability of received signals. Current trends in SDR development include integration with *artificial intelligence* (AI) and *machine learning* (ML) algorithms, which allow automatic adaptation of transmission parameters, such as modulation schemes or waveforms, to changing channel conditions [6, 7]. SDR also plays a key role in emerging communication standards such as *Long-Term Evolution* (LTE), *fifth-generation* (5G) *New Radio* (NR), and the upcoming *sixth-generation* (6G) systems [8, 9]. In parallel, this technology has found extensive applications in the field of vehicular communications and intelligent transportation systems, where reliability and frequency stability are critical to maintaining synchronization and ensuring safety [10, 11].

The versatility of SDRs has also led to their increasing use in metrology [12, 13], sensing [14–16], radar [17, 18], satellite communications [19–21], localization systems [22, 23], and electronic warfare [24, 25]. In many of these fields, especially those requiring precise time–frequency synchronization or accurate spectral analysis, frequency stability is a key performance factor [26, 27]. Even minor frequency fluctuations can affect the accuracy of synchronization, degrade signal integrity, or introduce phase noise – ultimately influencing the precision of the measurement and the reliability of the system.

The importance of frequency stability has been extensively discussed in metrological research [28–30], as it determines the applicability of SDR platforms in high-precision systems. However, *commercial off-the-shelf* (COTS) SDR devices are often characterised only by the accuracy of their internal oscillators, with little information on long-term or short-term stability. This limitation motivates empirical evaluation and modeling of SDR frequency stability to better understand its impact on practical applications.

In Part I of this study [31], we proposed a comprehensive measurement methodology to evaluate frequency stability on selected SDR platforms. The results obtained demonstrated significant differences in stability between various SDR models and highlighted the influence of an external *rubidium frequency standard* (RFS) on improving performance. Based on these experimental results, the present work focuses on developing mathematical models of SDR frequency instability that can be used directly in simulation studies.

Modeling the frequency instability of SDRs enables the prediction of real-world behavior in simulated environments, which is particularly valuable during the design and validation of the system. Accurate models allow engineers to evaluate the performance of synchronization algorithms, communication protocols, and measurement procedures prior to hardware implementation, thus reducing design costs and development time.

The main contributions of this paper are as follows:

- We propose a systematic methodology for modeling the frequency instability of the SDR based on experimentally measured data.
- We develop parametric models of frequency instability for selected SDR platforms.
- We provide ready-to-use models that can be applied directly in simulation environments to evaluate system performance under realistic conditions.

The remainder of the paper is organised as follows. Section 2 briefly discusses the principles of instantaneous frequency measurement in the time domain. Section 3 presents analysis of experimental data and methodology used to model SDR frequency instability. Section 4 provides conclusions and recommendations for future work.

Metrol. Meas. Syst., Vol. 32 (2025), No. 4, pp. 1–16
DOI: 10.24425/mms.2025.155811

2. Changes in Instantaneous Frequency in the Time Domain

The first part of the paper on the measurements [31] presents the testbed and methodology to obtain the instantaneous frequency measured in the baseband f_p as a function of time and to estimate the frequency stability parameters of SDRs. In addition, an example curve for the USRP-2930 radio is depicted. In this paper, Figs. 1 and 2 present instantaneous frequency changes for all tested SDRs measured for the carrier frequency of the transmitting signal (*i.e.*, from the signal generator – see [31]) at 1358 MHz and 5138 MHz, respectively. They constitute the basis for modeling frequency instability. The results presented were obtained for the acquisition time $t_A = 1$ s and the time step $\Delta t_A = 0.1$ s. The graphs illustrated on the left side of Figs. 1 and 2 were obtained for measures without an RFS in the receiving part of the testbed, whereas the graphs shown on the right side of these figures were determined with an RFS connected to the examined SDR.

Depending on the requirements of the designed systems, a different value of frequency stability is required. The influence of frequency stability on the accuracy of radio emitter localization was studied in [27, 32]. Considering the results obtained there and in this paper, a general conclusion can be drawn: the use of COTS SDR without a highly stable external clock does not ensure frequency stability at a sufficiently high level. The graphs presented on the left side of Figs. 1 and 2 show that the instantaneous frequency measured for SDR platforms changes significantly in the time domain. In the case of USRP N210 + RFX1200 and USRP-2930 for 1358 MHz, there are mainly instantaneous frequency fluctuations around a certain average value. In other cases, some trend of changes in the average frequency can also be observed in the measurement curves.

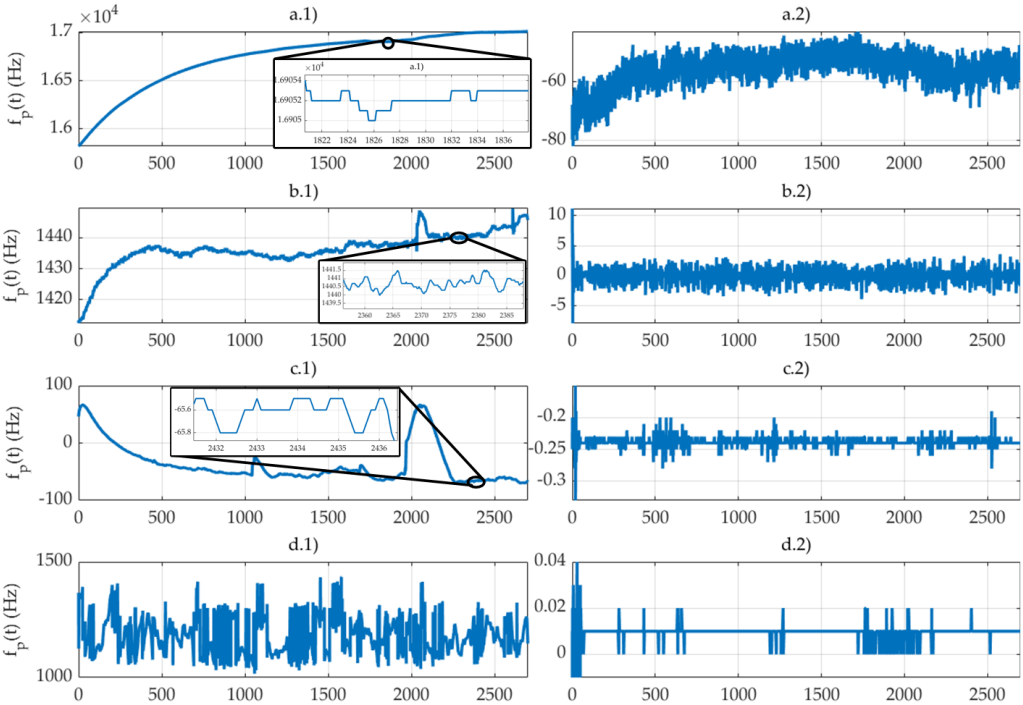

Fig. 1 continued on the next page

Fig. 1 continued from the previous page

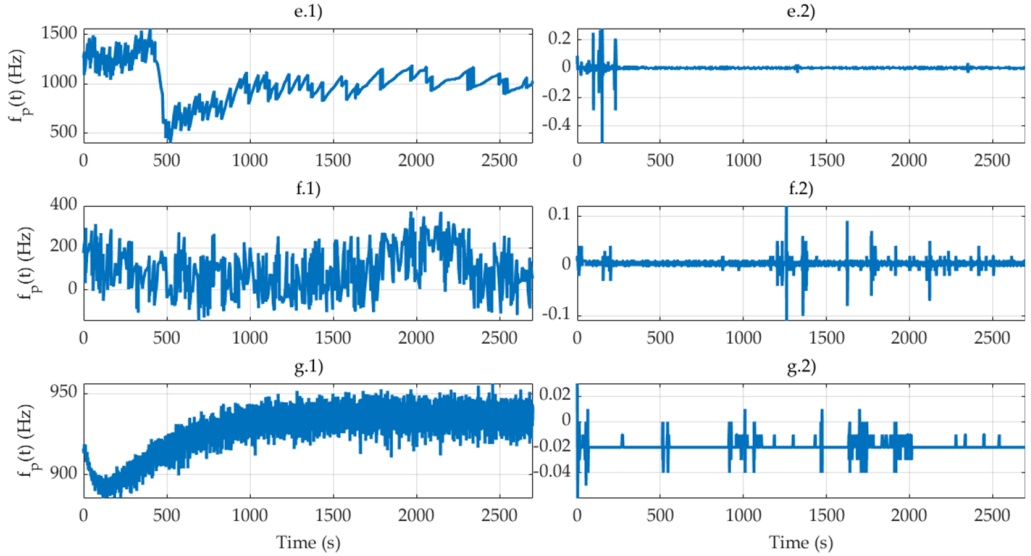

Fig. 1. Instantaneous frequency measured in the baseband f_p versus time (f = 1358 MHz, t_A = 1 s, Δt_A = 0.1 s) without an RFS (on left) and with an RFS (on right) for SDRs: (a) ADALM-PLUTO, (b) B200mini, (c) bladeRF 2.0 micro xA4, (d) USRP N210 + RFX1200, (e) USRP N210 + WBX, (f) USRP-2930, (g) USRP-2950R.

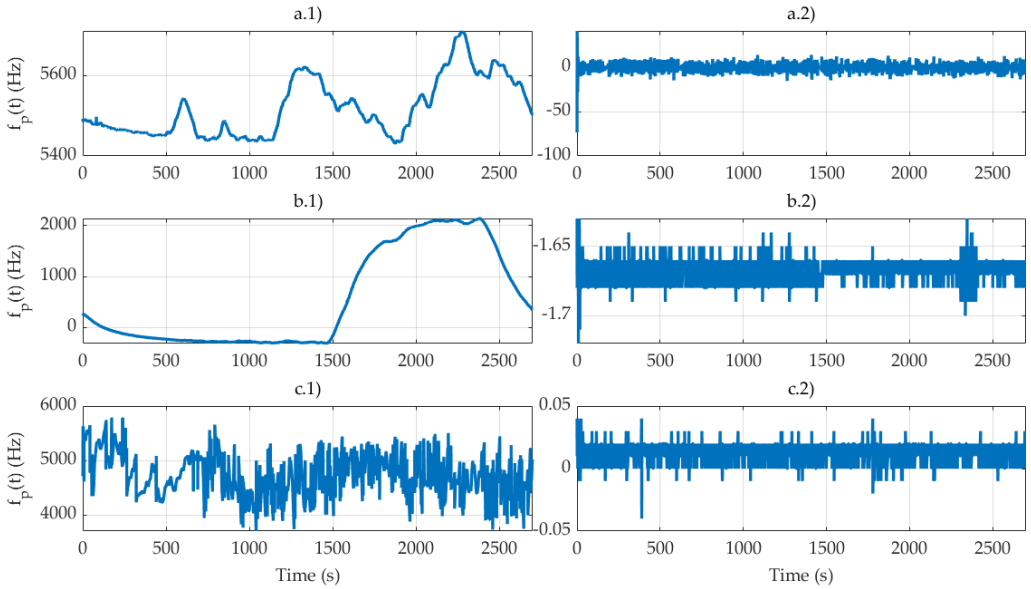

Fig. 2. Instantaneous frequency measured in the baseband f_p versus time (f = 5138 MHz, t_A = 1 s, Δt_A = 0.1 s) without an RFS (on left) and with an RFS (on right) for SDRs: (a) B200mini, (b) bladeRF 2.0 micro xA4, (c) USRP N210 + XCVR2450.

3. Analysis of measurement data for modeling SDR frequency instability

Modern techniques for testing the functionality of devices under various environmental conditions use simulation testing techniques that allow continuous verification of the developed solutions. Therefore, to assess the impact of instantaneous frequency instability on the correct functioning of devices using SDR, it is necessary to develop an appropriate simulation model that will reflect the actual frequency changes. Such a model allows one to perform tests for various measurements, not only for those resulting from a specific scenario. The practical implementation of measurement allows testing only for selected measurement scenarios. In addition, a single practical measurement requires setting up measurement testbeds, which involves significant time and work. An appropriate place, temperature, time, *etc.*, is often required, which cannot always be achieved.

For this reason, based on the results obtained, a method was proposed to model instantaneous frequency instability for the test-bed configurations presented in the first part of the paper [31]. It consists of several steps, which will be discussed later. In statistical measurements of the physical quantity $f_p(t)$, the measurement results are obtained in the form of time series [33]. Analyzing Fig. 1, we can see that the frequency fluctuations studied have a twofold nature. Fast $f_f(t)$ and slow $f_s(t)$ fluctuations are observed. The random value of the instantaneous frequency $f_p(t)$ can be represented as:

$$f_p(t) = f_f(t) + f_s(t) \tag{1}$$

Repeating the measurements over several consecutive days showed that slow changes (*i.e.*, trends) in frequency are of a deterministic nature for each type of equipment tested. On the other hand, the analysis of the frequency $f_f(t)$, which is obtained as a result of reducing the trend $f_f(t) = f_p(t) - f_s(t)$ in subsequent time intervals of length $\Delta_t = 5$ s, is the basis for assuming the random nature of this frequency component. Examples of results obtained for fast fluctuations $f_f(t)$ are shown on the right side of Fig. 3. In the adopted model, we assume that fast fluctuations $f_f(t)$ are a stationary normal process $N\left(0, \sigma_f\right)$, which can be described by one-dimensional *probability density function* (PDF) $g_f(f_f, \sigma_f)$:

$$g_f\left(f_f, \sigma_f\right) = \frac{1}{\sqrt{2\pi}\sigma_f} \exp\left(-\frac{f_f^2}{2\sigma_f^2}\right), \tag{2}$$

where σ_f is a standard deviation as a time-independent measure of instantaneous-frequency dispersion.

Therefore, the statistical model that represents the random frequency fluctuations of the SDR devices analysed describes the PDF $g_p(f_p, \sigma_f, t)$ as follows:

$$g_p\left(f_p, \sigma_f, t\right) = \frac{1}{\sqrt{2\pi}\sigma_f} \exp\left(-\frac{\left(f_p(t) - f_s\left(t\right)\right)^2}{2\sigma_f^2}\right) \tag{3}$$

Let $\mu_s(t)$ represent a function that approximates the slowly varying component of frequency fluctuations $f_s(t)$. The function $\mu_s(t)$ is determined based on data obtained throughout the measurement cycle according to the following criterion:

$$\mu_s(t) : \forall t \in \Delta_l, \quad \forall l = 1, 2, \ldots, L, E\left\{\left(\mu_s(t) - f_s(t)\right)^2\right\} = \min \to 0, \tag{4}$$

where: Δ_l is the lth time interval in which $f_p(t)$ is approximated, L is the number of time intervals determined in the entire measurement cycle, $E\{\cdot\}$ is the expectation operator analysed in each time interval Δ_l.

Table 1 presents the relationships approximating the slowly varying components $f_s(t)$ in accordance with conditions (4) for the analysed SDRs. The graphs of these functions in red are plotted against the background of the actual measurement data on the left side of Fig. 3. This allows for a visual comparison of the nature of the changes.

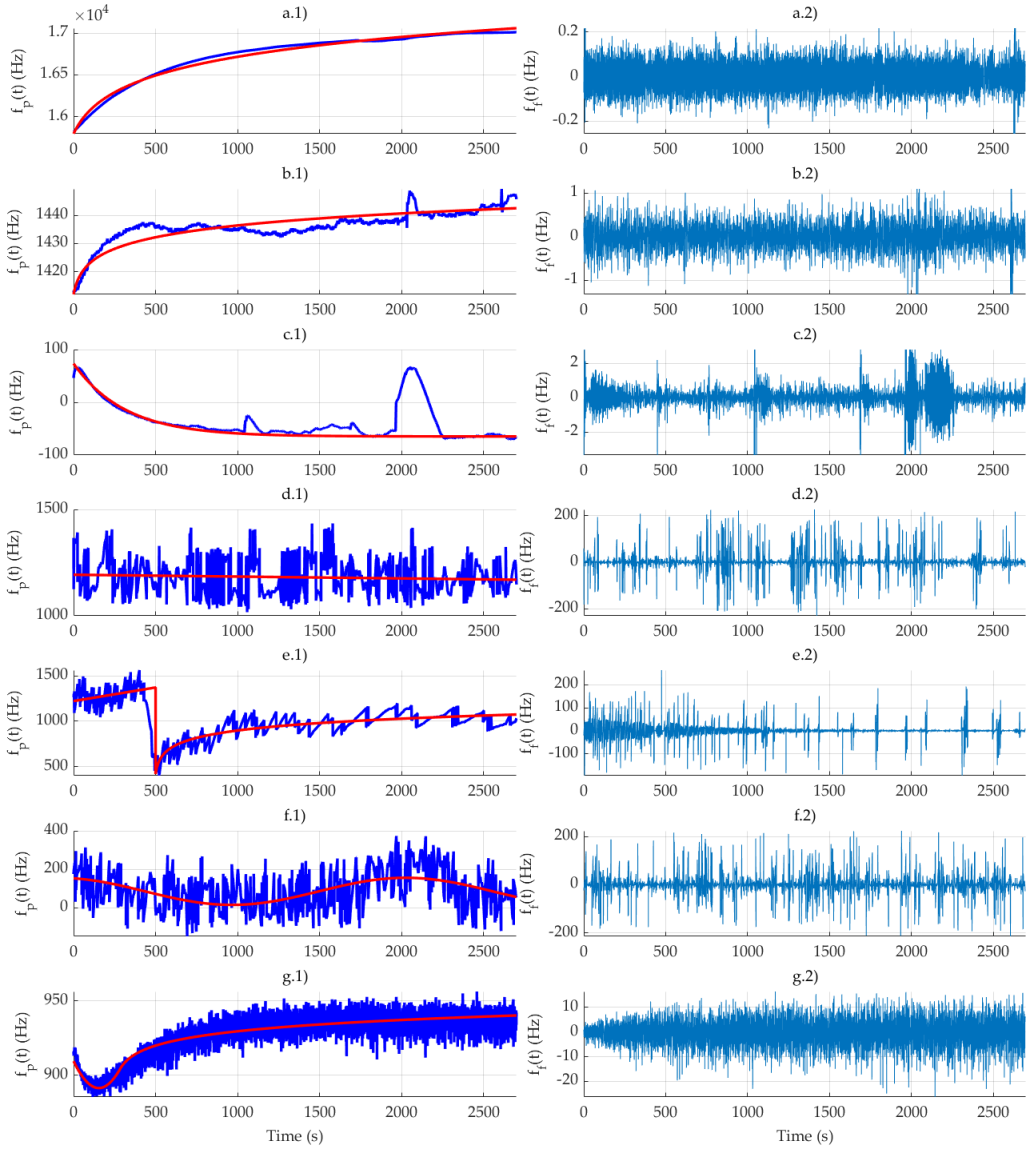

Fig. 3. Instantaneous frequency measured in the baseband versus time $f_p(t)$ with the designated approximating function $\mu_s(t)$ (on left) and after removing trend $f_f(t)$ (on right) (f = 1358 MHz, t_A = 1 s, Δt_A = 0.1 s, without an RFS) for SDRs: (a) ADALM-PLUTO, (b) B200mini, (c) bladeRF 2.0 micro xA4, (d) USRP N210 + RFX1200, (e) USRP N210 + WBX, (f) USRP-2930, (g) USRP-2950R.

Table 1. Relationships approximating slowly varying components of frequency fluctuations $f_s(t)$.

SDR	Approximating formula $\mu_s(t)$
ADALM-PLUTO	$\mu_s(t) = 363.34 \cdot \log(t + 858.63) + 13340.47$
B200mini	$\mu_s(t) = 6.26 \cdot \log(t + 201.09) + 1378.69$
bladeRF 2.0 micro xA4	$\mu_s(t) = 138.16 \cdot e^{-3.17 \cdot 10^{-4} \cdot t} - 64.75$
USRP N210 + RFX1200	$\mu_s(t) = -8.66 \cdot 10^{-4} \cdot t + 1192.94$
USRP N210 + WBX	$\mu_s(t) = \begin{cases} 0.03 \cdot t + 1221.61 \text{ for } 0 \le t < 5000 \\ 120.12 \cdot \log(t - 4907.93) - 128.44 \text{ for } t \ge 5000 \end{cases}$
USRP-2930	$\mu_s(t) = 70.36 \cdot \cos\left(2.97 \cdot 10^{-4} \cdot t + 0.28\right) + 85.60$
USRP-2950R	$\mu_s(t) = \begin{cases} 126 \cdot \cos\left(3.52 \cdot 10^{-4} \cdot t + 2.60\right) + 1017.52 \text{ for } 0 \le t < 2750 \\ 9.03 \cdot \log(t - 2370) + 848.84 \text{ for } t \ge 2750 \end{cases}$

After data detrending, we describe local oscillations using a normal PDF $N(0, \sigma_f)$ according to the assumption adopted. So, the standard deviation σ_f of the detrended data must be determined. To do this, first, the data is grouped in the form of a histogram representing the number M_i of frequency that occurred in ith bin. The resulting data are normalised by dividing M_i by the total number M of measurement data. So, the normalised histogram value m_i is defined for each bin:

$$m_i = \frac{M_i}{M}. \tag{5}$$

The frequency histogram determined from the measurement data allowed the calculation of σ_f. This parameter can be determined in two ways. In the first one, a deviation estimator σ_{fe} is determined based on the following simple relationship:

$$\sigma_{fe} = \sqrt{\sum_{i=1}^{I} m_i \cdot f_{fi}^2}, \tag{6}$$

where I is the total number of histogram bins and f_{fi} is the center of the ith bin.

Another way is to use the optimization procedure. In this case, the value of density $g_f\left(f_{fi}, \sigma_f\right)$ for center of the ith bin f_{fi} is estimated by the expression

$$\widetilde{g}\left(f_{fi}\right) = \frac{m_i}{\Delta_f}, \tag{7}$$

where $\widetilde{g}\left(f_{fi}\right)$ is the estimator of $g_f\left(f_{fi}, \sigma_f\right)$ for frequency f_{fi} and Δ_f is the width of the single bin.

So, in this case, determining optimal deviation with respect to minimizing mean square error comes down to solving the optimization problem in the form below:

$$\sigma_{fo} = \arg\min_{\sigma_f} S\left(\sigma_f\right) : S\left(\sigma_f\right) = \sum_{i=1}^{I} \left(\widetilde{g}\left(f_{fi}\right) - g_f\left(f_{fi}, \sigma_f\right)\right)^2. \tag{8}$$

By minimizing $S\left(\sigma_f\right)$, we found the fitted standard deviation σ_{fo}, for which $g_f\left(f_{fi}, \sigma_f\right)$ best approximates the frequency histogram expressed in the set of points $\left\{\left(f_{fi}, \widetilde{g}\left(f_{fi}\right)\right)\right\}$.

For the analysed SDRs, Table 2 presents σ_{fe} and σ_{fo} calculated based on the measurement data and relationships (6) and (8), respectively.

Table 2. Standard deviation σ_{fe} and σ_{fo} of the detrended data for the analysed SDRs.

SDR	**ADALM-PLUTO**	**B200mini**	**bladeRF**	**USRP N210+ RFX1200**	**USRP N210+ WBX**	**USRP-2930**	**USRP-2950R**
σ_{fe} [Hz]	0.049	0.274	0.332	7.432	4.865	12.832	4.682
σ_{fo} [Hz]	0.052	0.291	0.335	6.887	4.648	12.279	4.853

To assess the validity of the assumption that a normal PDF describes the fast frequency fluctuations, we used the chi-square statistical test. This test is widely used in statistics to test the normality of data distribution [34], however, its applications extend to a variety of other fields [35]. The normal PDF hypothesis was verified on subsets of the measurement data. Each subset consists of $Q = 270$ elements of f_f (*i.e.*, determined by the instantaneous frequencies after removing the trend). In this way, the influence of slow frequency changes on the verification result is eliminated. Histograms for an exemplary subset of the measurement data are shown in Figs. 4 and 5 for selected SDRs. Additionally, these figures present graphs of normal PDFs, determined for σ_{fe} and σ_{fo} and marked by blue and green lines, respectively. This presentation of results allows for a visual assessment of accuracy of approximation of the measurement data by the assumed PDF. We can see that the presented PDFs show high convergence with the approximated data. This is a promise for verifying the statistical properties of measurement data using a normal PDF.

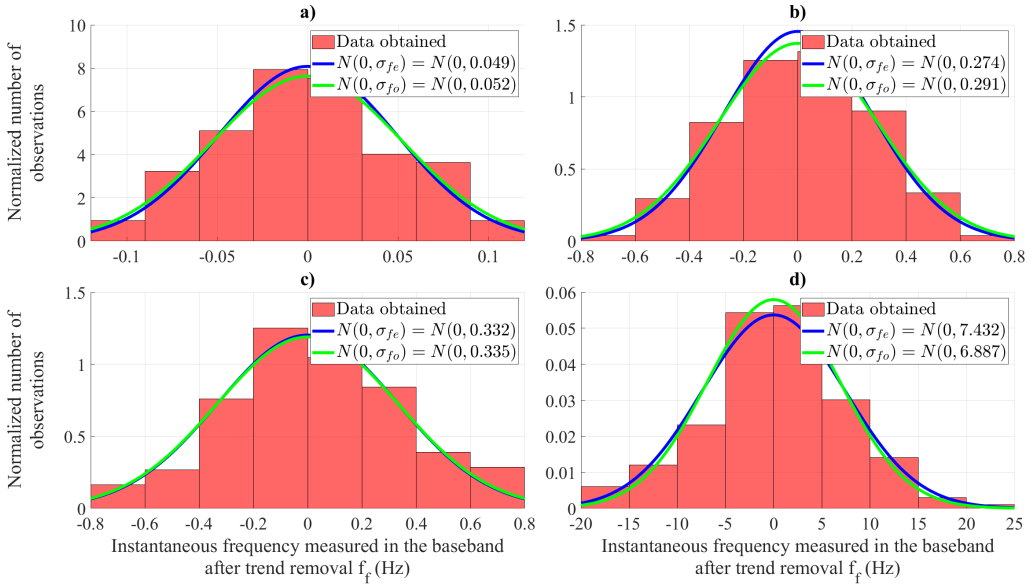

Fig. 4. Frequency histograms and approximating normal PDFs for SDRs: a) ADALM-PLUTO, b) B200mini, c) bladeRF 2.0 micro xA4, d) USRP N210 with an RFX1200 daughterboard.

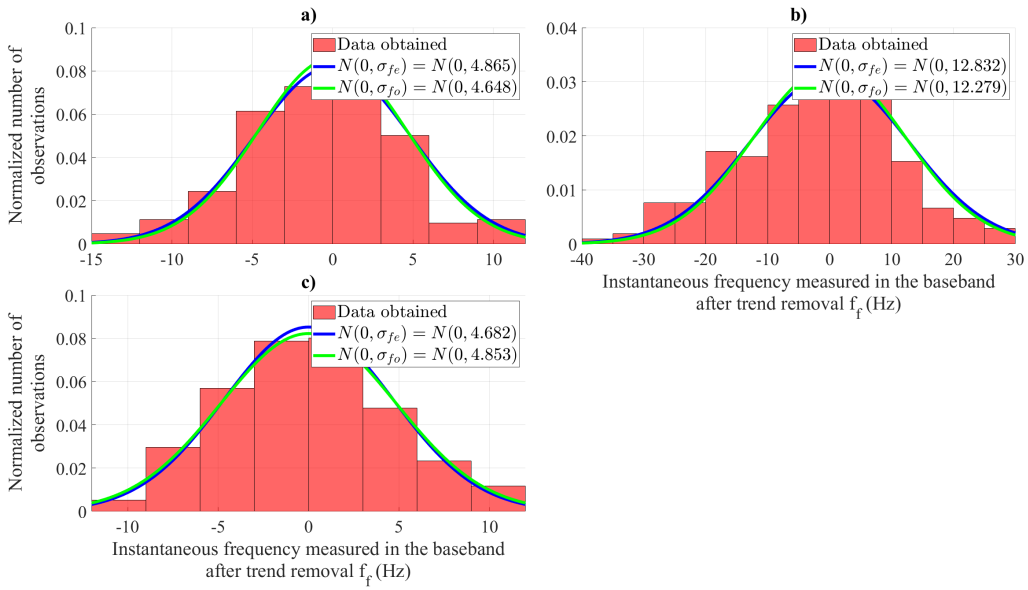

Fig. 5. Frequency histograms and approximating normal PDFs for SDRs: a) a USRP N210 radio with a WBX daughterboard, b) USRP-2930, c) USRP-2950.

The significance level α adopted for our study is 0.01. For hypothesis verification by this test the empirical value of the statistic X^2 is calculated according to the equation:

$$X^2 = \sum_{i=1}^{V} \frac{(n_i - Qp_i)^2}{Qp_i}, \tag{9}$$

where n_i is the number of frequencies in the ith bin for a single subset, p_i is a theoretical probability of frequency occurrence in the ith bin determined based on the normal PDF, V is the number of bins, Q is the number of the measured instantaneous frequencies f_p in each bin.

The critical value of 0.99 order quantile $\chi^2_{k,0.01}$ of the chi-squared PDF with $k = V - 3$ degree freedom constitutes a base for accepting the analysed hypothesis according to the dependency:

$$X^2 < \chi^2_{k,0.01}. \tag{10}$$

The test results for each SDR tested are summarised in Table 3.

Table 3. Chi-squared test results for the SDRs analysed.

SDR	$\chi^2_{k,0.01}$	X^2		$X^2 < \chi^2_{k,0.01}$	
		for σ_{fe}	**for** σ_{fo}	**for** σ_{fe}	**for** σ_{fo}
ADALM-PLUTO	15.086	6.684	5.484	True	True
B200mini	15.086	2.079	3.186	True	True
bladeRF 2.0 micro xA4	15.086	10.851	10.800	True	True
USRP N210 + RFX1200	16.812	5.953	9.315	True	True
USRP N210 + WBX	16.812	11.372	14.972	True	True
USRP-2930	24.725	15.262	20.137	True	True
USRP-2950R	15.086	4.044	3.358	True	True

It can be seen that for each case, a positive test result is obtained that confirms the normality of the distribution for all the data tested. Therefore, for a single curve that presents the instantaneous frequency $f_p(t)$ measured in the baseband versus time, the frequency instability can be modeled by providing a determined function $\mu_s(t)$ (see Table 1) and the PDF $f_f(t)$ reproducing the slow-changing and fast-changing component, respectively. The statistical properties of $f_f(t)$ describe a normal PDF with calculated σ_f (see Table 2) because this is justified by the verification results based on the chi-squared test. Example curves generated in this way are shown on the right side of Fig. 6. For comparison, the original data are shown on the left side of this figure.

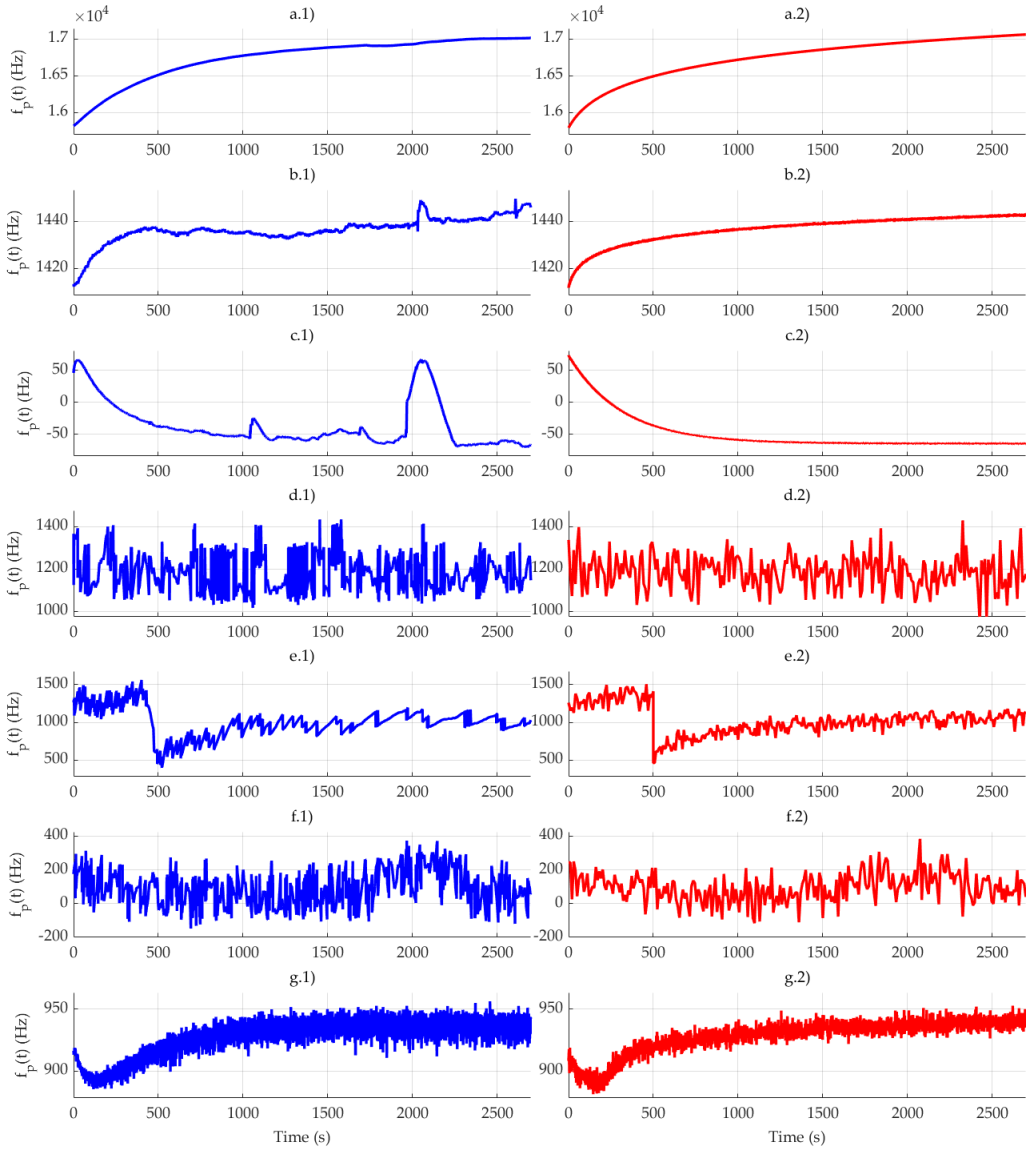

Fig. 6. Original data (on left) and the modeled curves (on right) of instantaneous frequency measured in the baseband f_p versus time (f = 1358 MHz, t_A = 1 s, Δt_A = 0.1 s, without an RFS) for SDR: (a) ADALM-PLUTO, (b) B200mini, (c) bladeRF 2.0 micro xA4, (d) USRP N210 + RFX1200, (e) USRP N210 + WBX, (f) USRP-2930, (g) USRP-2950R.

Analyzing Fig. 6, it can be seen that the obtained curves visually reflect the changes in the frequency of the original data very well. However, it was decided to use appropriate metrics to assess the accuracy of the modeled curves. It is worth recalling here that the curve of the instantaneous frequency measured in the baseband over time consists of both fast $f_f(t)$ and slow $f_s(t)$ fluctuations.

In the case of slow fluctuations $f_s(t)$, to assess the relative error in approximating the trend in the instantaneous frequency curves $f_p(t)$, it was necessary to use an additional metric. That metric allowed us to assess the accuracy of the approximation of the instantaneous frequency curves $f_p(t)$ using the approximating functions $\mu_s(t)$ presented in Table 1. A frequently used metric in journals is the *root mean square error* (RMSE) [36]. In our case, we additionally normalised it [37] by dividing the RMSE by the range of changes defined by the maximum and minimum values of the instantaneous frequency f_p. In this way, we use the *normalised RMSE* (NRMSE) δ expressed by the following formula:

$$\delta[\%] = \frac{\sqrt{\dfrac{1}{Q \cdot V} \sum\limits_{j=1}^{Q \cdot V} \left(\mu_s\left(t_j\right) - f_p\left(t_j\right)\right)^2}}{\left|f_{p\,\max} - f_{p\,\min}\right|} \cdot 100, \tag{11}$$

where $f_{p\,\max}$ and $f_{p\,\min}$ are the maximum and minimum of the instantaneous frequency f_p, respectively, and $j = 1, 2, \ldots, Q \cdot V$ is the index of the selected instantaneous frequency f_p.

To assess the accuracy of the fast fluctuations $f_f(t)$ distribution estimation (see Figs. 4 and 5), the Kolmogorov–Smirnov statistic D is used in the form as in [38]:

$$D = \sup_f \left|F_m(f) - F_f(f)\right|, \tag{12}$$

where $F_m(f)$ and $F_f(f)$ are the empirical and theoretical *cumulative distribution functions* (CDFs), respectively, and f is the center value of the subsequent frequency ranges for the histograms shown in Figs. 4 and 5.

The evaluation results for approximation accuracy of slow fluctuations $f_s(t)$ and the estimation of fast fluctuations $f_f(t)$ distributions are presented in Table 4.

Table 4. Results for approximation accuracy of slow fluctuations $f_s(t)$ and estimation of fast fluctuations $f_f(t)$ distributions for the analysed SDRs.

SDR	**ADALM-PLUTO**	**B200mini**	**bladeRF**	**USRP N210+ RFX1200**	**USRP N210+ WBX**	**USRP-2930**	**USRP-2950R**
δ [%]	3	8	22	19	10	16	9
D	0.135	0.126	0.110	0.129	0.160	0.148	0.137

The evaluation of slow and fast frequency fluctuations performed shows differences in their representation accuracy. Regarding slow fluctuations, the representation of frequency changes across the tested SDR platforms shows significant differences. The best accuracy for slow frequency fluctuations $f_s(t)$ approximation (δ metric), was obtained for ADALM-PLUTO ($\delta \approx 3\%$) and B200mini ($\delta \approx 8\%$), while bladeRF results gave the largest RMSE ($\delta \approx 22\%$). In the case of the bladeRF and USRP N210+RFX1200 platforms, obtaining small approximation errors is hindered by large, random frequency changes in the time domain, which are shown in Fig. 6c.1) and d.1),

whereas for fast fluctuations $f_f(t)$, all D statistics are limited to the range from 0.11 to 0.16. This indicates statistical convergence of the results of the developed representation of fast frequency fluctuations for all tested platforms. Therefore, the obtained results are satisfactory and indicate that it is possible to use an appropriate model to perform simulation studies for various measurement scenarios, not limited to the one used for model development.

4. Conclusions

The conducted research and analyses have shown that frequency instability in common SDRs can be reliably represented in simulation conditions by dividing it into a slowly changing component (trend) and a fast-changing component (fast fluctuations represented by a stationary process with a normal distribution). This approach allows for taking into account both long-term frequency drift and short-term fluctuations in the systems under study.

The results of the analyses can be useful in designing and verifying solutions based on SDR in various areas, such as radio communication, location systems, radio spectrum monitoring, and sensor systems. The presented model allows for easy generation of signals in simulations burdened with a characteristic type of frequency instability, which significantly facilitates testing new algorithms and solutions. The ability to conduct repeatable and controlled experiments in a simulation environment significantly reduces the costs and time needed to verify projects, especially compared to extensive tests in real conditions. In the future, methods may be developed to consider additional environmental factors (*e.g.*, temperature fluctuations) and integration with advanced radio system design tools.

Acknowledgements

This work was developed within the framework of the research project on "Command and control of group of COMINT radio-electronic reconnaissance unmanned aerial vehicles based on modern IT technologies", with the acronym UAV-COMINT, no. DOB-SZAFIR/01/B/029/03/2021, sponsored by the National Center for Research and Development (NCBR), Poland, under the 3/SZAFIR/2021 program, and grant no. UGB/22-059/2025/WAT, sponsored by the Military University of Technology (WAT), Poland.

References

[1] Goeller, L., & Tate, D. (2014). A technical review of software defined radios: vision, reality, and current status. In *2014 IEEE Military Communications Conference* (pp. 1466–1470). https://doi.org/10.1109/milcom.2014.242

[2] Machado-Fernández, José Raúl. (2015). Software Defined Radio: Basic Principles and Applications. *Revista Facultad de Ingeniería*, 24(38), 79–96. Retrieved December 12, 2025, from http://www.scielo.org.co/scielo.php?script=sci_arttext&pid=S0121-11292015000100007&lng=en&tlng=en

[3] Krishnan, R., Babu, R. G., Kaviya, S., Kumar, N. P., Rahul, C., & Raman, S. S. (2017). Software defined radio (SDR) foundations, technology tradeoffs: A survey. *2017 IEEE International Conference on Power, Control, Signals and Instrumentation Engineering (ICPCSI)*, 2677–2682. https://doi.org/10.1109/icpcsi.2017.8392204

[4] Michailidis, E. T., Maliatsos, K., & Vouyioukas, D. (2024). Software-defined radio deployments in UAV-driven applications: A comprehensive review. *IEEE Open Journal of Vehicular Technology*, 1–43. https://doi.org/10.1109/ojvt.2024.3477937

[5] Hussain, W., Isoaho, J., & Nurmi, J. (2016). The Future of Software-Defined Radio: Recommendations. In *Springer eBooks* (pp. 237–238). https://doi.org/10.1007/978-3-319-49679-5_12

[6] Jdid, B., Hassan, K., Dayoub, I., Lim, W. H., & Mokayef, M. (2021). Machine Learning Based Automatic Modulation Recognition for Wireless Communications: A Comprehensive Survey. *IEEE Access*, *9*, 57851–57873. https://doi.org/10.1109/access.2021.3071801

[7] de la Rosa, J. M. (2022). AI-Assisted Sigma-Delta Converters – Application to Cognitive Radio. *IEEE Transactions on Circuits & Systems II: Express Briefs*, *69*(6), 2557–2563. https://doi.org/10.1109/tcsii.2022.3161717

[8] Manco, J., Dayoub, I., Nafkha, A., Alibakhshikenari, M., & Thameur, H. B. (2022b). Spectrum Sensing Using Software Defined Radio for Cognitive Radio Networks: A survey. *IEEE Access*, *10*, 131887–131908. https://doi.org/10.1109/access.2022.3229739

[9] Skokowski, P., Malon, K., & Łopatka, J. (2022). Building the Electromagnetic Situation Awareness in MANET Cognitive Radio Networks for Urban Areas. *Sensors*, *22*(3), 716. https://doi.org/10.3390/s22030716

[10] Lahoud, C., Ehsanfar, S., Gabriel, M., Kuffner, P., & Mosner, K. (2022). Experimental Testbed Results on LTE/5G-V2I Communication Using Software Defined Radio. *ICC 2022 – IEEE International Conference on Communications*, 2894–2899. https://doi.org/10.1109/icc45855.2022.9838411

[11] Zhang, J., Lu, K., Wan, Y., Xie, J., & Fu, S. (2024). Empowering UAV-Based Airborne Computing Platform with SDR: Building an LTE Base Station for Enhanced Aerial Connectivity. *IEEE Transactions on Vehicular Technology*, 1–14. https://doi.org/10.1109/tvt.2024.3406339

[12] Andrich, C., Ihlow, A., Bauer, J., Beuster, N., & Del Galdo, G. (2018). High-Precision measurement of sine and pulse reference signals using Software-Defined radio. *IEEE Transactions on Instrumentation and Measurement*, *67*(5), 1132–1141. https://doi.org/10.1109/tim.2018.2794940

[13] "Software defined radio market size |industry report, 2030." Accessed: Apr. 09, 2025. [Online]. Available: https://www.grandviewresearch.com/industry-analysis/software-defined-radio-sdr-market

[14] Deprez, K., Colussi, L., Korkmaz, E., Aerts, S., Land, D., Littel, S., Verloock, L., Plets, D., Joseph, W., & Bolte, J. (2023). Comparison of low-cost 5G electromagnetic field sensors. *Sensors*, *23*(6), 3312. https://doi.org/10.3390/s23063312

[15] Ferrari, P., Flammini, A., & Sisinni, E. (2011). New architecture for a wireless smart sensor based on a software-defined radio. *IEEE Transactions on Instrumentation and Measurement*, *60*(6), 2133–2141. https://doi.org/10.1109/tim.2011.2117090

[16] Xu, Y., Amineh, R. K., Dong, Z., Li, F., Kirton, K., & Kohler, M. (2022). Software Defined Radio-Based Wireless Sensing System. *Sensors*, *22*(17), 6455. https://doi.org/10.3390/s22176455

[17] Capria, A., Saverino, A. L., Giusti, E., & Martorella, M. (2023). SDR-based passive radar technology. In *Passive Radars on Moving Platforms* (pp. 265–289). https://doi.org/10.1049/sbra536e_ch9

[18] Feng, W., Friedt, J., & Wan, P. (2021). SDR-Implemented Ground-Based Interferometric Radar for Displacement Measurement. *IEEE Transactions on Instrumentation and Measurement*, *70*, 1–18. https://doi.org/10.1109/tim.2021.3069805

[19] Grenier, A., Lei, J., Damsgaard, H. J., Quintana-Ortí, E. S., Ometov, A., Lohan, E. S., & Nurmi, J. (2024). Hard SyDR: a Benchmarking Environment for Global Navigation Satellite System Algorithms. *Sensors*, *24*(2), 409. https://doi.org/10.3390/s24020409

[20] Majoral, M., Arribas, J., & Fernández-Prades, C. (2024). Implementation of a High-Sensitivity Global Navigation Satellite System Receiver on a System-on-Chip Field-Programmable Gate Array Platform. *Sensors*, *24*(5), 1416. https://doi.org/10.3390/s24051416

[21] Platonov, A. (2019). Perfect SDR transmitters with feedback for small satellites and their metrological characteristics. *Measurement*, *152*, 106578. https://doi.org/10.1016/j.measurement.2019.04.063

[22] Codău, C., Buta, R., Păstrăv, A., Dolea, P., Palade, T., & Puschita, E. (2024). Experimental evaluation of an SDR-Based UAV localization system. *Sensors*, *24*(9), 2789. https://doi.org/10.3390/s24092789

[23] Goverdovsky, V., Yates, D. C., Willerton, M., Papavassiliou, C., & Yeatman, E. (2016). Modular Software-Defined Radio Testbed for Rapid Prototyping of Localization Algorithms. *IEEE Transactions on Instrumentation and Measurement*, *65*(7, 1577–1584. https://doi.org/10.1109/tim.2016.2540998

[24] Ferreira, R., Gaspar, J., Sebastião, P., & Souto, N. (2022). A Software Defined Radio Based Anti-UAV Mobile System with Jamming and Spoofing Capabilities. *Sensors*, *22*(4), 1487. https://doi.org/10.3390/s22041487

[25] Chiper, F., Martian, A., Vladeanu, C., Marghescu, I., Craciunescu, R., & Fratu, O. (2022). Drone Detection and Defense Systems: Survey and a Software-Defined Radio-Based Solution. *Sensors*, *22*(4), 1453. https://doi.org/10.3390/s22041453

[26] Szczepanik, R., & Kelner, J. M. (2025b). Filtering and overlapping data for accuracy enhancement of Doppler-based location method. *Sensors*, *25*(5), 1465. https://doi.org/10.3390/s25051465

[27] Bednarz, K., Wojtuń, J., Kelner, J. M., & Różyc, K. (2024). Frequency Instability Impact of Low-Cost SDRs on Doppler-Based Localization Accuracy. *Sensors*, *24*(4), 1053. https://doi.org/10.3390/s24041053

[28] Mochizuki, K., Uchino, M., & Morikawa, T. (2007b). Frequency-Stability Measurement System Using High-Speed ADCs and Digital Signal Processing. *IEEE Transactions on Instrumentation and Measurement*, *56*(5), 1887–1893. https://doi.org/10.1109/tim.2007.895588

[29] de la Rosa, J. J. G., Moreno, A., Lloret, I., Pallarés, V., & Liñán, M. (2006b). Characterisation of frequency instability and frequency offset using instruments with incomplete data sheets. *Measurement*, *39*(7), 664–673. https://doi.org/10.1016/j.measurement.2006.01.001

[30] Marszalec, M., Lusawa, M., & Osuch, T. (2020c). Efficient frequency jumps detection algorithm for atomic clock comparisons. *Metrology and Measurement Systems*, *28*(2021)(1), pp. 107–121. https://doi.org/10.24425/mms.2021.135996

[31] Bednarz, K., Wojtuń, J., Kelner, J. M., Ziółkowski, C., & Leśnik, C. (2025). Frequency stability of software-defined radios – part I. Measurements. *Metrology and Measurement Systems*, *32*(3), 1–18. https://doi.org/10.24425/mms.2023.155803.

[32] Kelner, J. M., Ziółkowski, C., & Marszałek, P. (2016b). Influence of the frequency stability on the emitter position in SDF method. In *International Conference on Military Communications and Information Systems (ICMCIS)* (Vol. 60, pp. 1–6). https://doi.org/10.1109/icmcis.2016.7496554

[33] Przystupa, K., Kolodiy, Z., Yatsyshyn, S., Majewski, J., Khoma, Y., Petrovska, I., Lasarenko, S., & Hut, T. (2022). Standard deviation in the simulation of statistical measurements. *Metrology and Measurement Systems*, *30*(1), 17–30. https://doi.org/10.24425/mms.2023.144403

[34] Crane, R. B., Malila, W. A., & Richardson, W. (1972). Suitability of the normal density assumption for processing multispectral scanner data. *IEEE Transactions on Geoscience Electronics*, *10*(4), 158–165. https://doi.org/10.1109/tge.1972.271285

[35] Catelani, M., Zanobini, A., & Ciani, L. (2010). Uncertainty interval evaluation using the Chi-square and Fisher distributions in the measurement process. *Metrology and Measurement Systems*, *17*(2), 195–204. https://doi.org/10.2478/v10178-010-0017-5

[36] Lewicka, O. (2023). Method for accuracy assessment of topo-bathymetric surface models based on geospatial data recorded by UAV and USV vehicles. *Metrology and Measurement Systems*, *30*(3), 461–480. https://doi.org/10.24425/mms.2023.146421

[37] Liu, L., Xu, S., Tang, J., Guan, K., Griffis, T. J., Erickson, M. D., Frie, A. L., Jia, X., Kim, T., Miller, L. T., Peng, B., Wu, S., Yang, Y., Zhou, W., Kumar, V., & Jin, Z. (2022). KGML-ag: a modeling framework of knowledge-guided machine learning to simulate agroecosystems: a case study of estimating N_2O emission using data from mesocosm experiments. *Geoscientific Model Development*, *15*(7), 2839–2858. https://doi.org/10.5194/gmd-15-2839-2022

[38] Ziółkowski, C., & Kelner, J. M. (2016). Empirical Models of the Azimuthal Reception Angle — Part I: Comparative analysis of empirical models for different propagation environments. *Wireless Personal Communications*, *91*(2), 771–791. https://doi.org/10.1007/s11277-016-3496-1

Kacper Bednarz was born in Poland in 1997. He graduated from the Military University of Technology (WAT) in 2022 as the top student of the Faculty of Electronics, obtaining an M.Sc. degree in electronics and telecommunications. In 2023 he began his studies at the WAT Doctoral School. From 2022 he has worked as an engineer at the Institute of Communication Systems, Faculty of Electronics, Military University of Technology. He is also a junior vice-chair of the F Commission on Wave Propagation and Remote Sensing of the Polish National Committee of the International Union of Radio Science – URSI. The scope of his scientific activity covers digital signal processing, wireless communications, software-defined radio (SDR) technology, localization techniques, and sensing. As part of the Group of the Analysis, Modelling, and Estimation of Radio Channels (GAME-RC), he is the contractor of four research projects on tactical radio reconnaissance from unmanned aerial vehicles (UAVs), command and management of a radio-electronic reconnaissance UAV group, and long-range communications.

Jan M. Kelner (Member, IEEE) received his M.Sc. degree (Hons.) in applied physics, a Ph.D. degree in telecommunications, and an MBA degree in cybersecurity management from the Military University of Technology (WAT), Warsaw, Poland, in 2001, 2011, and 2024, respectively, and the D.Sc. (habilitation) degree in information and communication technology from the AGH University of Science and Technology, Krakow, Poland, in 2020. He is currently an Associate Professor with the Institute of Communications Systems, Faculty of Electronics, WAT, where he started to work in 2003. From 2021 to 2024, he was the Institute Director. Since September 2024, he has been the Faculty Dean. From 2017 to 2024, he was a Principal Voting Member of the Information Systems Technology Panel Operating within the NATO Science and Technology Organization. He has been an Expert with the European Defence Agency (EDA) CapTech Information and the Office of Electronic Communications, since 2019 and 2022, respectively. Since 2001, he has been involved in many research and development projects for the Ministry of National Defence, the EDA, the National Centre for Research and Development, and the National Science Centre. He is also the Manager of four research projects and the Supervisor for twelve Ph.D. students. He has authored or co-authored more than 270 articles in peer-reviewed journals and conferences. He is a reviewer for 35 scientific journals and about 20 conferences. His current research interests include wireless communications, modelling and measurements of radio channels, quality of services in mobile networks, electronic warfare, localization techniques, counter-unmanned aircraft systems.

Jarosław Wojtuń received his B.Sc. and M.Sc. degrees in electronics and telecommunications and his Ph.D. in digital signal processing from the Military University of Technology, Warsaw, Poland, in 2009, 2011, and 2021, respectively. He is currently an Assistant Professor and the Deputy Director of the Institute of Communications Systems of the Faculty of Electronics, Military University of Technology (WAT). His research focuses on digital signal processing, wireless communications, modelling and measurements of radio channels, and localization techniques.

Czesław Leśnik received his M.Sc. (E.E.) degree in electronics and the Ph.D. and D.Sc. degrees in telecommunications from the Military University of Technology (WAT), Warsaw, Poland, in 1978, 1999, and 2018, respectively. Since 1981, he has been employed with the Institute of Radioelectronics, Faculty of Electronics, WAT, where he has been an Associate Professor since 2018. His professional activity focuses on radar theory and techniques, and signal processing.

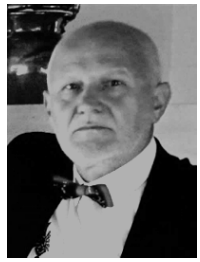

Cezary Ziółkowski received his M.Sc. degree in telecommunications engineering from the Military University of Technology (WAT), Warsaw, Poland, in 1978, the M.Sc. degree in mathematics (specialty—applied mathematical analysis) from the University of Warsaw, in 1989, and the Ph.D. degree in telecommunications engineering and the D.Sc. (habilitation) degree in radio communications from WAT, in 1993 and 2013, respectively. From 1982 to 2013, he was a researcher and lecturer at the Faculty of Electronics, WAT, where he has been an Associate Professor since 2013. He was involved in many research projects, especially in the fields of radio communications systems engineering, radio wave propagations, radio communication network resources management, and electromagnetic compatibility in radio communication systems. He is the author or the co-author of more than 200 scientific articles and research reports.